05750-16-P

THE UNIVERSITY OF MICHIGAN

COLLEGE OF ENGINEERING
Department of Chemical and Metallurgical Engineering
Department of Mechanical Engineering

Fifth Quarterly Progress Report

INVESTIGATION OF LIQUID METAL BOILING HEAT TRANSFER

Richard E. Balzhiser
Project Director

Robert E. Barry
Bruce F. Caswell
Herman Merte, Jr.
Andrew Padilla, Jr.

ORA Project 05750

under contract with:

FLIGHT ACCESSORIES LABORATORY
AERONAUTICAL SYSTEMS DIVISION
AIR FORCE SYSTEMS COMMAND
UNITED STATES AIR FORCE
WRIGHT-PATTERSON AIR FORCE BASE, OHIO
CONTRACT NO. AF 33(657)-11548

administered through:

OFFICE OF RESEARCH ADMINISTRATION ANN ARBOR

September 1964

"To expedite dissemination of information, this report is being forwarded for your information prior to review and approval by the ASD project officer and is, therefore subject to change. Any comments which you may have should be forwarded to ASD (Mr. Charles L. Delaney), Wright-Patterson AFB, Ohio, within 15 days of receipt to insure correction of errors before final approval is given."

FOREWORD

This report summarizes progress during the period May 15, 1964 to September 15, 1964 on Contract AF 33(657)-11548. This contract provides for continuation of the experimental programs initiated under the original contract between the University of Michigan and ASD. The investigation is being conducted in the Liquid Metals Laboratory of the Department of Chemical and Metallurgical Engineering. Professor Richard E. Balzhiser is serving as Project Director at the University of Michigan. Messrs. Barry, Caswell and Padilla, all graduate students in chemical engineering are responsible for specific portions of the program.

Progress on the agravic studies with boiling mercury will be summarized in these reports. This work is being conducted by Professor Herman Merte, Jr. and Mr. Samuel Walker in the Mechanical Engineering Department.

Mr. Charles L. Delaney is project engineer for ASD.

ABSTRACT

No additional burnout data has been obtained during this period. The equipment modification has been completed and rubidium will be charged during the next period.

A numerical analysis of the edge effects in the 1" diameter film boiling apparatus has been completed. The uncertainty in condensing coefficients for sodium beneath the plate makes it difficult to correct for the large amount of heat which flows up the wall when the system operates in the film regime. A design for a modified boiler is presented.

The forced convection apparatus was reassembled after the zirconium chips in the hot trap were replaced. Filters were added at several points in the system to collect suspended solids or oxide if either existed in the system. Despite all efforts plugs still developed and flow was obtained for only brief periods during this time. The extremely small pumping restriction seems to accentuate the problem and consideration is being given to purchasing a new pump which might permit circulation for a period sufficiently long to collect all solids in the loop filters.

The agravic apparatus was operated with mercury at a/g of one. Data was obtained in the nucleate, transition and film regimes.

TABLE OF CONTENTS

List of Figures vi

Pool Boiling Studies. 1

Film Boiling. 6

Forced Circulation Studies. 21

Liquid Metal Boiling in Agravic Fields. 24

Appendix I. 33

LIST OF FIGURES

1. Piping Details 2

2. Location of Guard Heaters #1 - #5 4

3. Location of Thermocouples #1 - #9 4

4. Rubidium Charging System 5

5. Model for Analysis of Boiling Plate 8

6. Calculated Temperature Field for Boiling Plate in Film Boiling Regime 10

7. Comparison of Actual Boiling Surface Flux and Flux Calculated from Measured Data 12

8. Effect of Boiling Coefficient 13

9. Effect of Condensing Coefficient 15

10. Test Section for Proposed 3" Diameter Boiler 17

11. Model for Analysis of Proposed 3" Diameter Boiler 18

12. Analysis of Design Parameters for Proposed 3" Diameter Boiler 20

13. Forced Circulation Loop 22

14. Thermocouple Locations for Reference 25

15. Time-Temperature Data 26

16. Time Temperature Data 29

17. Boiling Data for Mercury 31

18. Procedure for Calculating Tube Wall Temperatures 38

19. Postulated Boiling Curve for Assigning Inside Tube Wall Boiling Coefficients 39

20. Longitudinal Variation of Wall Temperature 40

Pool Boiling - Bruce F. Caswell

The pool boiling equipment has been extensively modified during the past summer. The system has been completely repiped as shown in Figure 1. The new piping system is built of 316 stainless steel tubing with welded connections wherever possible. All threaded connections are made up with Teflon tape. Jamesbury high vacuum ball valves are used as shown. The pressure gauge is an Ashcroft laboratory test gauge with a range of 0-300 psig and an accuracy of 1/2% of full scale. It has been calibrated against a mercury column at increments of one inch of mercury. A cylinder of helium is connected to the system as shown in Figure 1. According to the manufacturer (Matheson Company) it has a combined oxygen and water content of less than 5 ppm. Our analysis by mass spectrometer was made but is in doubt as to sampling procedure and other sources of inaccuracy in this low range. The piping system has been checked for leaks while under vacuum by means of a Consolidated Electrodynamics type 24-210 helium leak detector which is sensitive to 1 part helium in 300,000 parts of air and which will measure a leak rate of 10^{-8} atm cc/sec. For this system this leak rate corresponds to 0.01 micron/hour at 1 micron pressure. The system was checked at the most sensitive setting on the detector and all detectable leaks have been eliminated. A vacuum of 0.1 micron can be obtained on the process side of the system. While under vacuum the system has been heated and outgassed for several days in order to remove adsorbed gases. A flame was applied to the vacuum manifold and to other lines to promote desorption. Some difficulty was encountered in sealing the 3/8" NPT connection of the boiling tube. Several sealing compounds were tried and a MoS_2-oil mixture was finally found to be satisfactory.

Four boiling tubes have been fabricated. However, two of these, when installed, gave excessive electrical resistance due to contact surfaces not

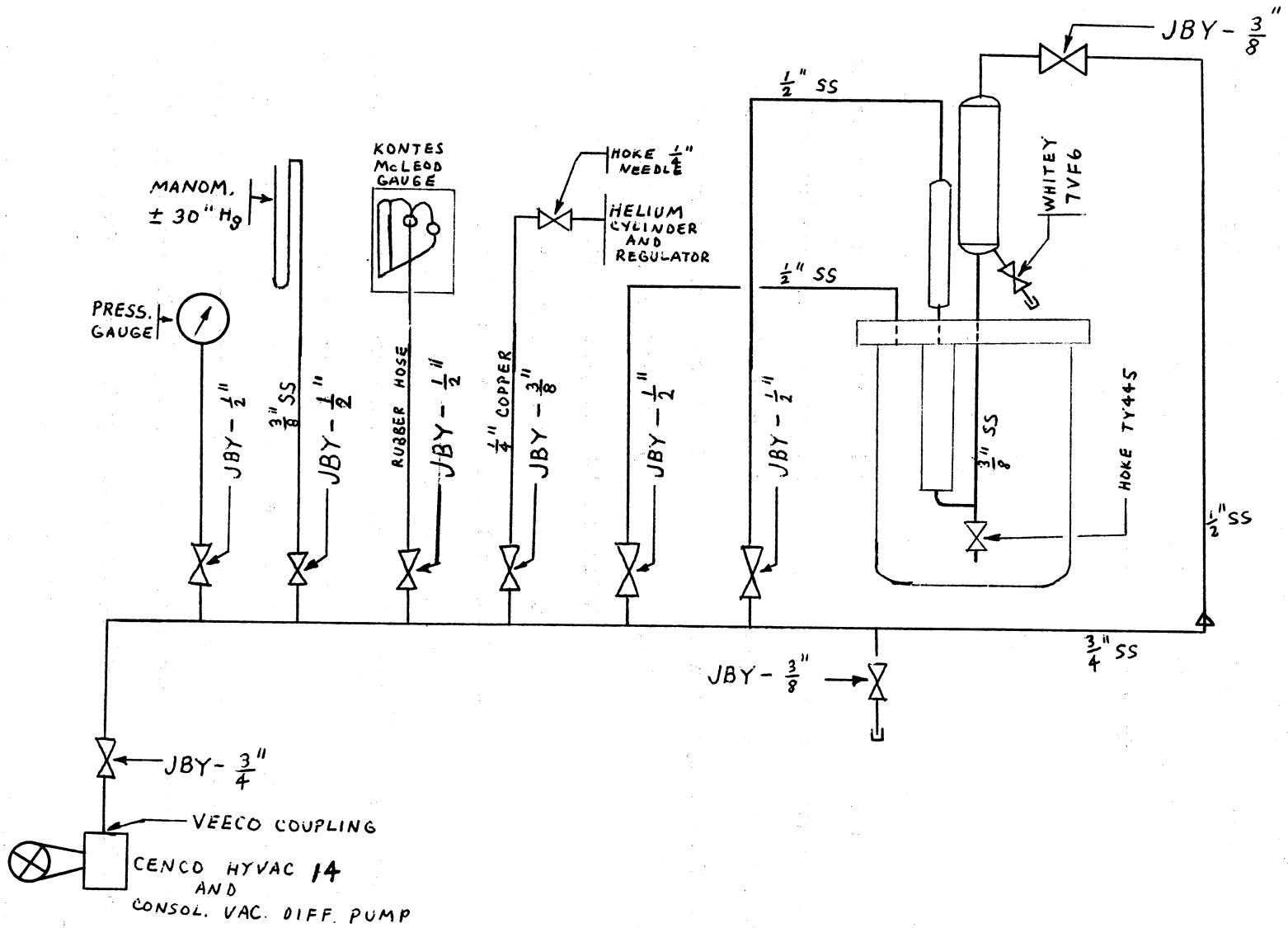

Figure 1. Piping Details

meeting properly. One has been installed now which is satisfactory in this respect. It was found that a thin layer of oxide on the molybdenum rod increased the contact resistance several fold. This was eliminated by placing the rod in a holder and polishing the surface on a metallographic wheel.

Nine thermocouples have been placed at various locations around the boiling vessel as shown in Figure 3. These temperatures will be recorded and should provide control points for the guard heaters. Five guard heaters have been installed as shown in Figure 2. These are made of Hevi-Duty type 505 KSP heating coils, good to 2200°F, wrapped in asbestos. Each heater is 500 watts capacity. These heaters are controlled with variable transformers and are adjusted during a run to minimize heat losses from the boiling vessel.

The three thermocouples on the surface of the boiling tube each are connected to a Leeds and Northrup Speedomax H recorder with a response time of one second full scale. Each recorder has an alarm circuit which will shut off the power to the boiling tube if a temperature excursion occurs. The alarm circuits are wired in series so that any single one can shut down the main power.

A modified charging system has been designed and installed as shown in Figure 4. As shown, the shipping container is connected to the bottom of the boiling vessel. After charging, the shipping container and valves B and C are disconnected from the system. Valve A remains inside the outer jacket of the system. If desired, due to some difficulty with the system, the contents of the boiling vessel can be transferred to the vessel above the flange without removing the outer jacket or making any connections to the system.

The adjustable thermocouple which is used to measure the bulk liquid temperature is now being calibrated, after which rubidium will be charged and burnout data will be taken.

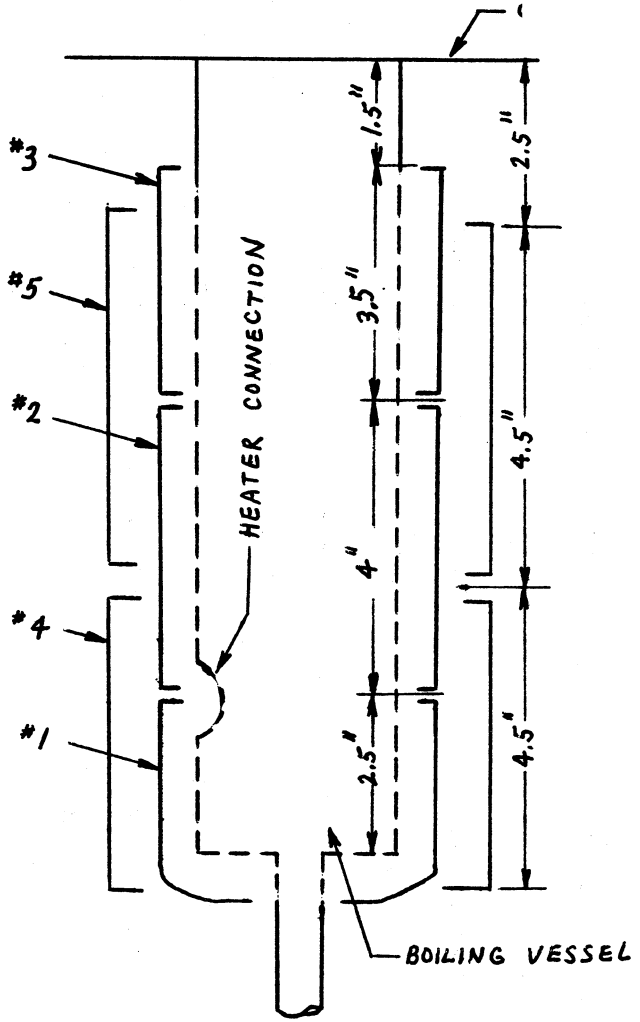

Figure 2. Location of Guard Heaters #1 - #5

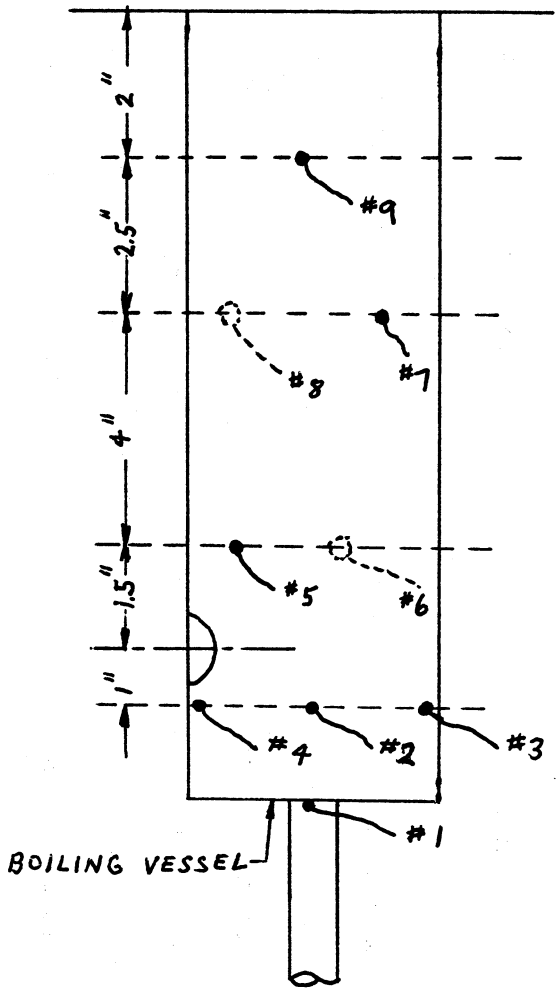

Figure 3. Location of Thermocouples #1 - #9

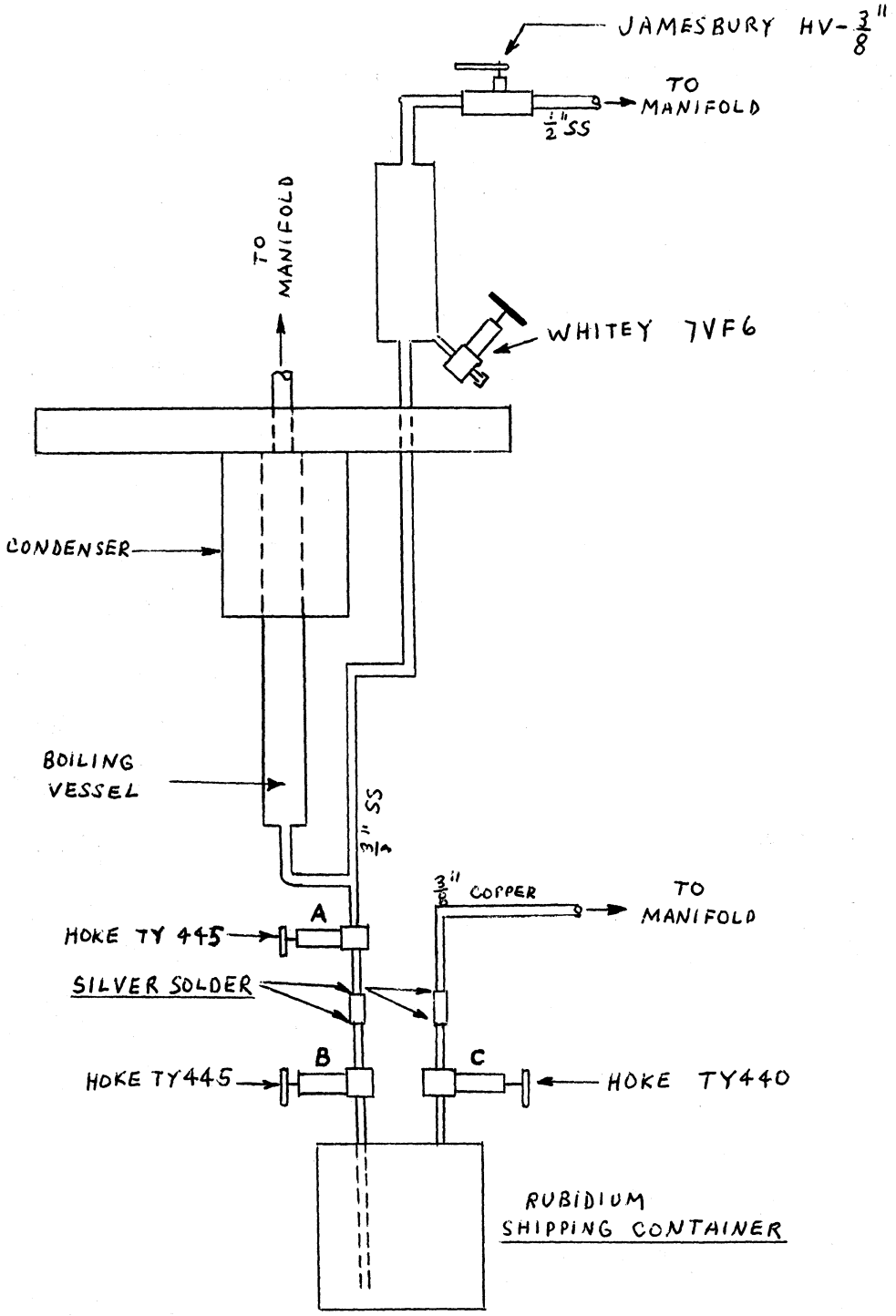

Figure 4. Rubidium Charging System

Film Boiling - Andrew Padilla

It had previously been determined that the boiling instabilities encountered during operation were due to nucleation difficulties in the bottom sodium chamber. Superheating of the sodium was followed by loud knocks indicating vapor generation which gave rise to brief periods of stable boiling. The difficulty in nucleating and the decay of stable boiling may have been associated with a high level of non-condensable gases at the condensing surface. To alleviate this problem, a hot finger was designed to act as a nucleation source. Concurrently, an extensive effort was begun to predict quantitatively the heat-transfer data which would be obtained under a variety of stable operating conditions.

The hot finger consisted of a 1/8" OD tantalum-sheathed swaged assembly containing a single insulated tantalum wire. The current was to pass up through the wire and down through the sheath and liquid metal to the vessel which would be grounded. The tip of the hot finger was to be 1/16" OD containing a smaller diameter wire than the lead section and would be immersed in the liquid. Bubble generation from the tip of the hot finger would prevent superheating of the heated walls of the sodium chamber. A fitting was designed to handle the insertion of the hot finger and a thermocouple to the sodium chamber and to allow for charging the system. The small diameter of the entrance to the chamber prevented the allowance for removal of non-condensable gases. Three quotations for the proposed hot finger were received. However, it was decided that modification of the present system to avoid the operational difficulties previously encountered was not feasible due to the results of the analysis of the test section.

The mathematical analysis of the test section is an extension to three dimensions of the calculations in the Third Quarterly Report. It involves the solution of the finite-difference form of Laplace's equation in

cylindrical coordinates using the IBM 7090 computer. Figure 5 shows the actual dimensions of the boiling plate and the location of the micro-thermocouple holes. The model used for the analysis uses a boiling and condensing surface of 1.0 inch diameter instead of the actual 0.98 inch.

The detailed formulation of the finite-difference equations and the application of the appropriate boundary conditions are treated in Appendix I. The program allows for a constant condensing and boiling coefficient along the bottom and top of the boiling plate respectively and for radiation from the outer wall to a shield at constant temperature. Since the inside tube wall immediately above the boiling plate must pass from film boiling through transition and nucleate boiling to natural convection whenever the top surface of the plate is in film boiling, a variable boiling coefficient along the inside tube wall is used. This assignment of boiling coefficients is based on a heat balance on small increments of length along the tube wall. By postulating a boiling curve, the heat transfer rate and temperature along the length of the wall can be calculated, thus determining the coefficients. This calculation and the procedure to determine the appropriate length of wall required for different operating conditions are also discussed in Appendix I.

In the present experimental system, the heat flux at the boiling surface must be calculated by measuring the temperature at several points in the boiling plate using micro-thermocouples. The temperature measurements are then used with the known distance between thermocouples and the thermal conductivity to establish the heat flux across the plate. This heat flux is equal to the flux at the boiling surface only if no radial gradients exist. The boiling plate contains thermocouples at three different depths in the boiling plate to measure the temperature gradient across the plate and at two different radii to detect any radial heat flow.

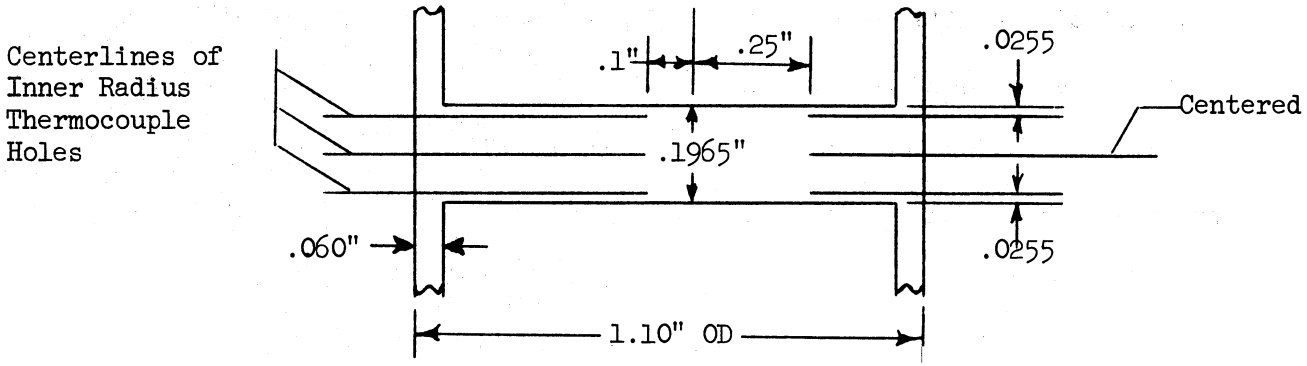

BOILING PLATE

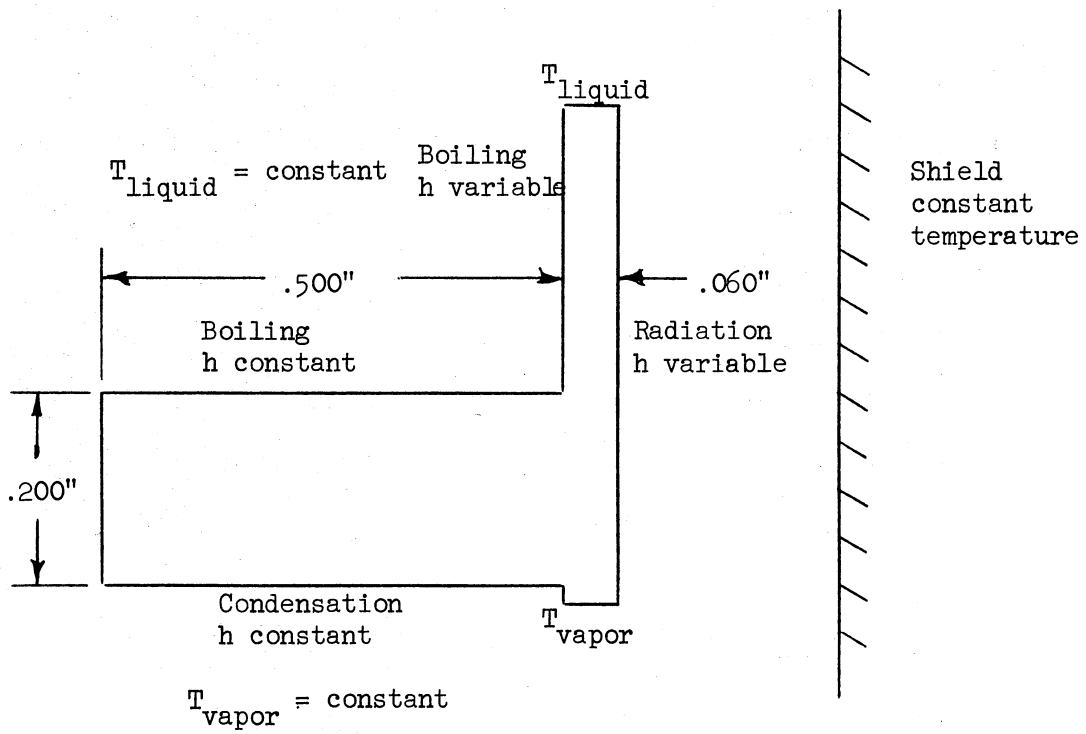

MODEL FOR ANALYSIS

Figure 5. Model for Analysis of Boiling Plate

The boiling plate is connected to a tube which serves as the containment vessel for the boiling liquid. The flux lines in the boiling plate depend on the relative resistances to heat flow of the boiling surface and axial conduction up the tube wall. If the boiling coefficient is very low, as in film boiling, then the relatively low resistance to heat flow by axial conduction up the walls of the tube distorts the flux lines in the plate. This radial heat flow causes a radial temperature variation along the boiling surface. Also, the axial temperature gradient in the boiling plate is no longer an accurate indication of the flux occurring at the boiling surface. The relation between the boiling surface flux and the flux calculated by measuring the axial temperature profile in the plate is quite complicated and requires the determination of the temperature field in the boiling plate for the set of desired operating conditions.

The computer program for the test section determines the temperature field in the boiling plate and the tube wall immediately above the boiling plate. The temperatures along the top surface of the plate can then be used with the assumed boiling coefficient to calculate the radial variation in the boiling surface flux. By taking the temperatures at two different depths below the boiling surface, the radial variation in the "measured flux" can also be calculated. For the cases which follow, this measured flux is based on temperatures .020 inch below the boiling surface and .020 inch above the condensing surface (.160 inch apart) and on the thermal conductivity of columbium-1% zirconium.

Figure 6 shows the temperature field for a film-boiling coefficient of 100 Btu/hr-ft^2-°F and a condensing coefficient of 5000 Btu/hr-ft^2-°F. The boiling coefficients along the inside tube wall immediately above the boiling plate were assigned according to the procedure discussed in Appendix I. It is noticed that the isotherms are severely distorted, especially at the

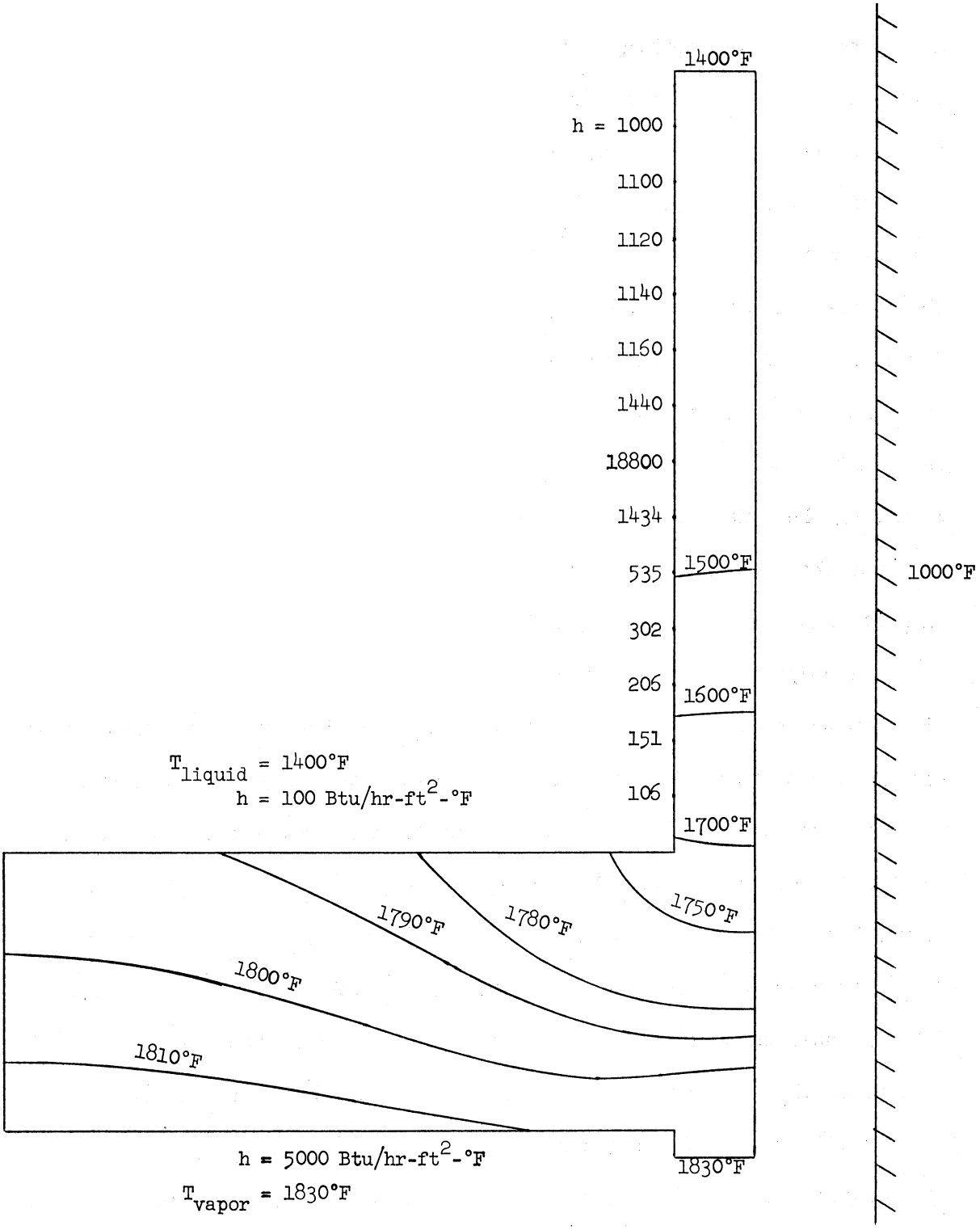

Figure 6. Calculated Temperature Field for Boiling Plate in Film Boiling Regime

junction of the boiling plate and the tube wall where axial conduction up the tube wall affords a low resistance to heat transfer in comparison with the low film-boiling coefficient. Figure 7 summarizes the results which can be calculated from Figure 6. Hence, if two thermocouples, one .020 inch below the boiling surface and the other .020 inch above the condensing surface, were used to calculate a "measured flux," this flux would be considerably higher than the flux actually occurring at the boiling surface. This measured flux would be 37% higher at the center of the boiling plate and would increase to over six times the boiling surface flux at the inside tube wall. However, the thermocouples in the actual boiling plate are located at .10 inch and .25 inch from the centerline, and the errors for these radii are 41% and 66% respectively.

The distortion of the flux lines (which are perpendicular to the isotherms) due to axial conduction up the tube wall depends very strongly on the boiling coefficient. The ratio of the measured flux and the boiling surface flux can be plotted as a function of the radial distance from the center of the boiling plate. Figure 8 compares this ratio for the entire range of possible boiling coefficients. The boiling coefficients of 50, 100, and 200 Btu/hr-ft^2-°F represent the range of expected film-boiling coefficients. The coefficients of 2,000 and 20,000 Btu/hr-ft^2-°F represent probable transition- and nucleate-boiling coefficients, respectively. The analysis shows that very small error can be expected during transition and nucleate boiling. In the high nucleate-boiling regime, the very high value of the boiling coefficient represents a lower resistance to heat transfer than axial conduction up the tube wall and the flux lines are slightly distorted towards the boiling plate near the outside of the boiling plate. If a film boiling coefficient as high as 200 Btu/hr-ft^2-°F is possible, then the error between the measured flux and boiling surface flux is 15% at the

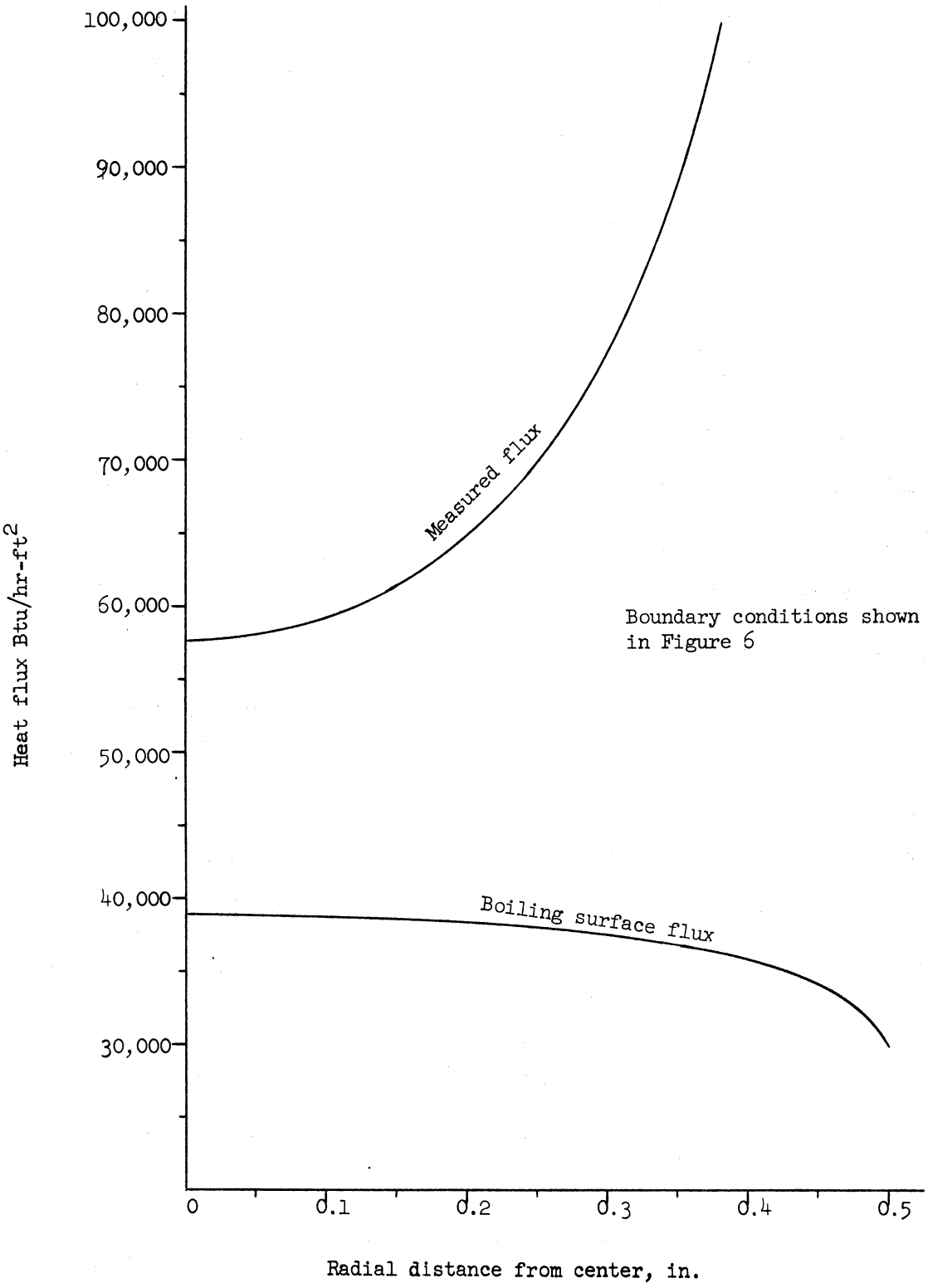

Figure 7. Comparison of Actual Boiling Surface Flux and Flux Calculated from Measured Data

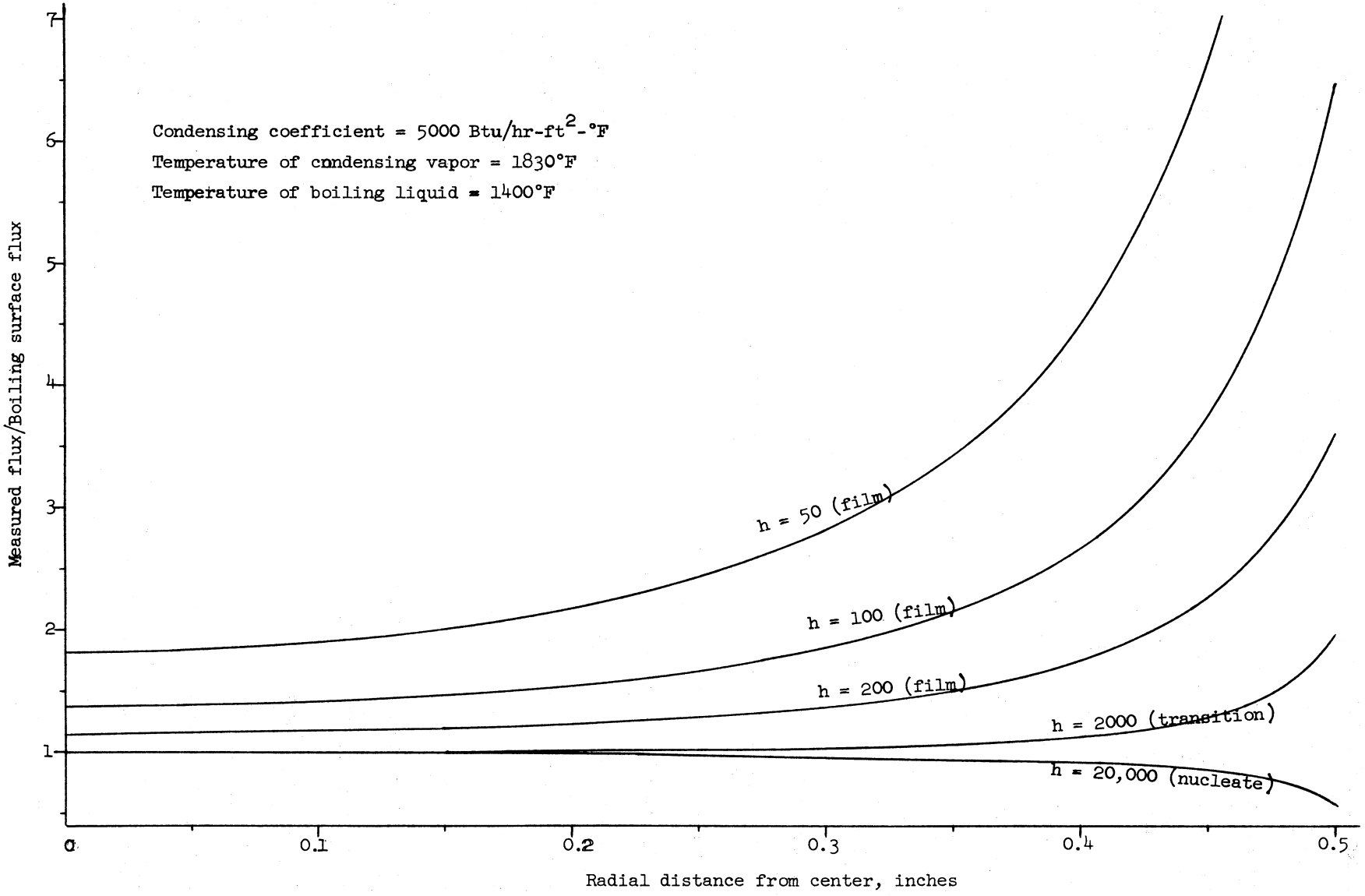

Figure 8. Effect of Boiling Coefficient

centerline and 28% at a distance of .25 inch from the centerline. However, a low film-boiling coefficient of 50 Btu/hr-ft^2-°F introduces an error of 82% at the center of the boiling plate which increases to 140% at the location of the thermocouples at the outer radius in the actual boiling plate.

The results are also sensitive to the value of the condensing coefficient. Figure 9 shows the radial variation of the ratio of measured flux to boiling surface flux for condensing coefficients of 500, 1,000, and 10,000 Btu/hr-ft^2-°F keeping the boiling coefficient constant at 100 Btu/hr-ft^2-°F. At the center of the boiling plate, the respective errors are 5%, 24%, and 33%. Hence, by increasing the condensing coefficient during film boiling a larger fraction of the energy is driven up the tube walls rather than across the boiling plate.

The temperature of the radiation shield was not found to be an important parameter. This is due to the low value of the pseudo-convection coefficient due to radiation in comparison to boiling and condensing coefficients. As an example, a tube wall temperature of 2000°F radiating to a radiation shield at 1000°F has a pseudo-convection coefficient of 24 Btu/hr-ft^2-°F. Since heat transfer due to radiation depends on the fourth power of the absolute temperature, the temperature of the radiating surface is much more important than that of radiation shield. This also indicates that guard heaters along the outside of the boiling tube would be relatively ineffective in cutting down the heat losses due to axial conduction up the tube walls.

Therefore, the film boiling condition for which the experimental system was primarily designed would produce the largest error in any heat-transfer results. Reasonably good data might be obtained in the transition- and nucleate-boiling regimes. The resulting error would be very sensitive to the value of the boiling and condensing coefficients over which there is no control. Any correction for experimental error would involve the deter-

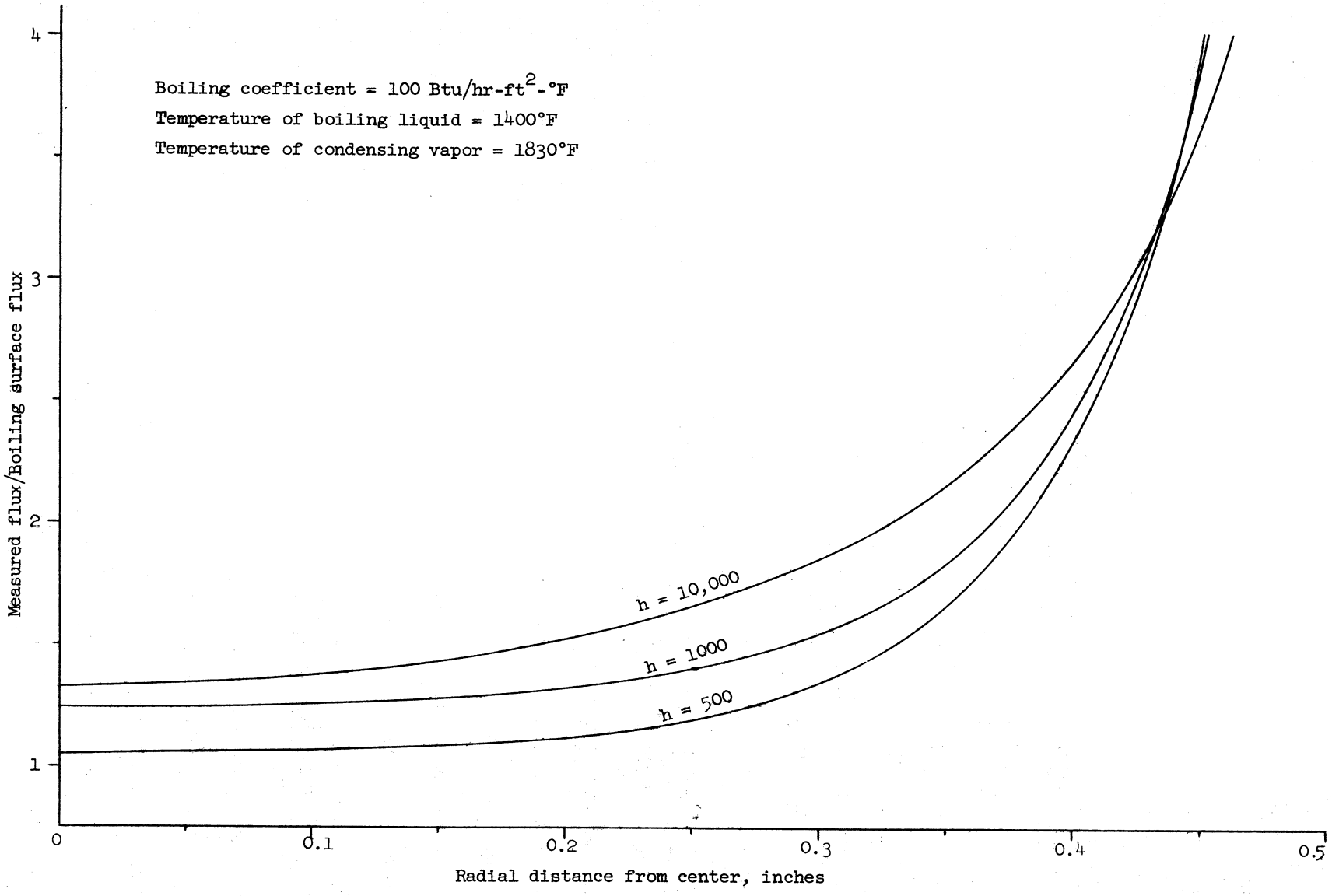
Boiling coefficient = 100 Btu/hr-ft^2-°F
Temperature of boiling liquid = 1400°F
Temperature of condensing vapor = 1830°F
h = 10,000
h = 1000
h = 500
Measured flux/Boiling surface flux
Radial distance from center, inches
0
0.1
0.2
0.3
0.4
0.5
1
2
3
4

mination of the coefficients sought and their use in a complicated analysis of the type just discussed. The convection for film use in a complicated analysis of the type just discussed. The correction for film boiling would be considerable and at least of the same magnitude as the true value of film-boiling coefficients. It seems improbable that this system can be modified to avoid these difficulties.

The original purpose in using a condensing media as the heat source was to avoid the possibility of burnout. However, there are indications that a block heater using cartridge-type heaters, as in the agravic pool-boiling studies of Clark and Merte, possesses sufficient thermal capacity to avoid failure of the boiling surface in passing from nucleate to film boiling. In addition, experience with the high-flux pool boiler has shown the reliability of its graphite heater in withstanding very high temperatures and surface fluxes. This has resulted in the design of a 3-inch diameter boiler which is shown in Figure 10. The heater flock of Mo-0.5 Ti is to be joined to the containment vessel, consisting of 3-inch Schedule 40 Haynes-25 pipe machined from the outside diameter to a .060" wall thickness, in a tongue-in-groove configuration giving a 3.068-inch diameter boiling surface.

The heater units will consist of .160" diameter by 1" long graphite rods inside of .180" OD by .160" ID boron nitride sleeves. The six units will be staggered on two different diameters. Current will pass in through three elements in parallel at one radius, through the block, and out through the units at the other radius.

Considerable analysis has also been carried out to determine the operating characteristics of the proposed design. Figure 11 shows the model used for the analysis which is very similar to that for the present system. The condensing boundary condition is replaced by the assumption of constant temperature at the bottom, which represents some finite distance above the

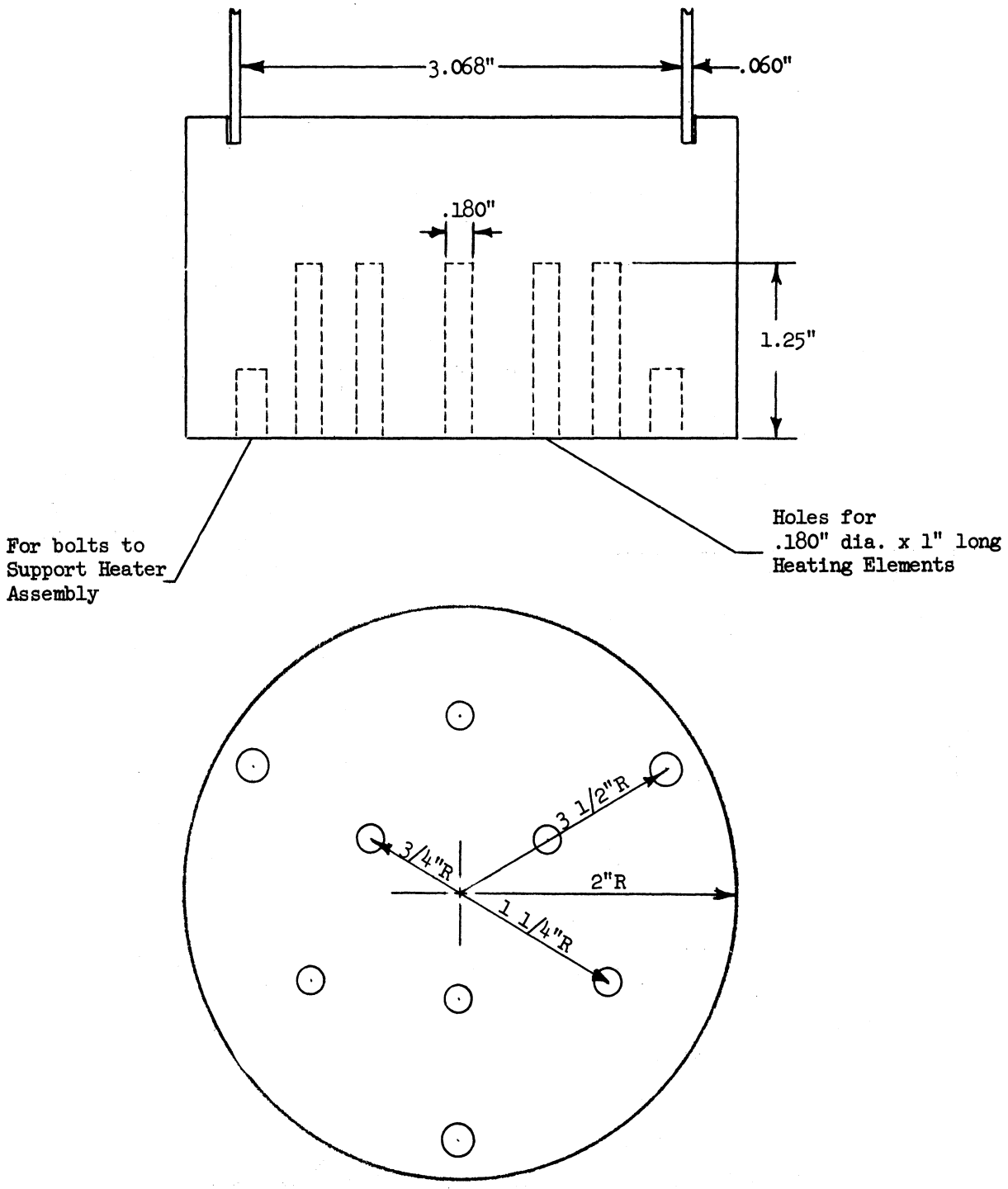

Figure 10. Test Section for Proposed 3" Diameter Boiler

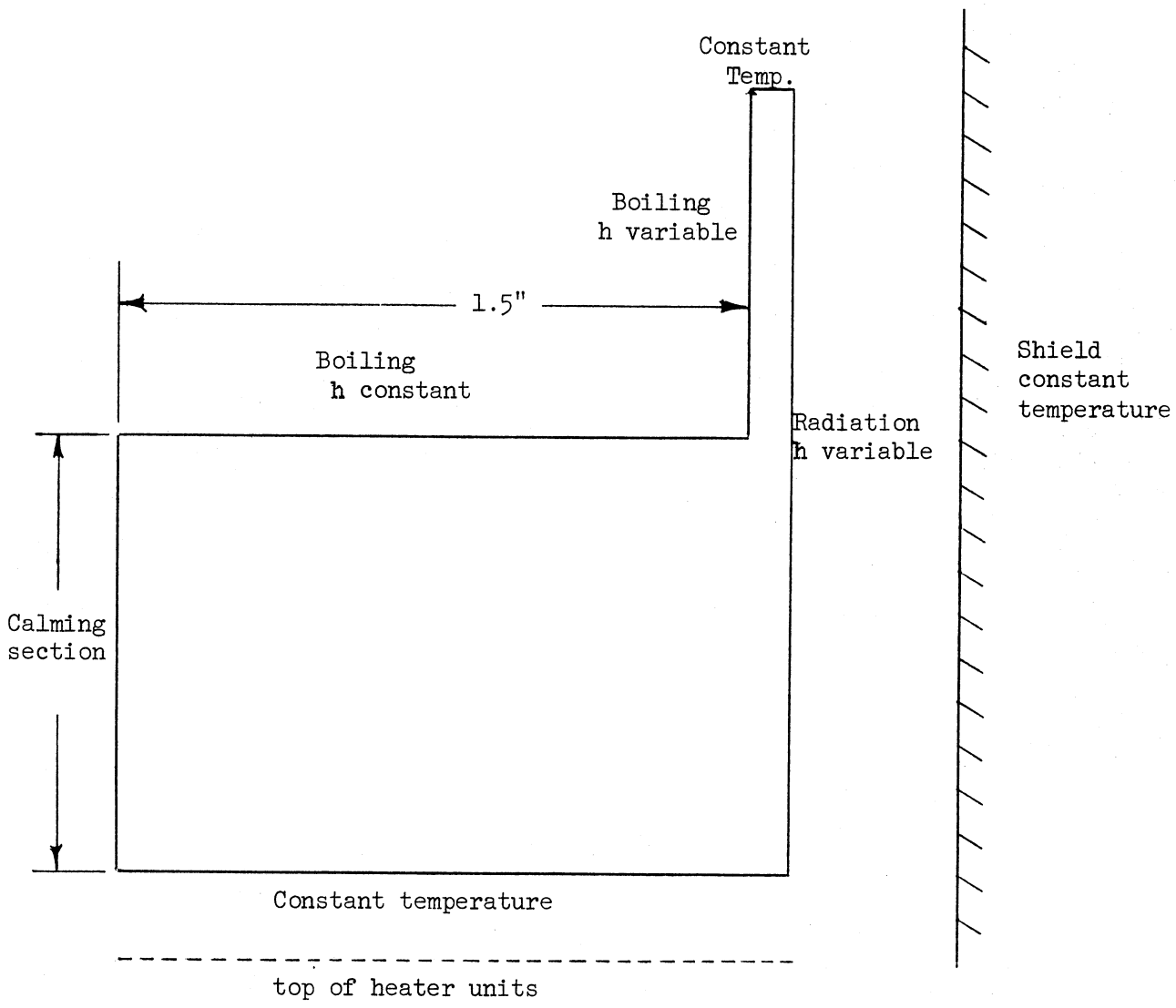

Figure 11. Model for Analysis of Proposed 3" Diameter Boiler

top level of the heater units. The other boundary conditions remain the same. However, the program allows for the difference in thermal conductivity of the block and the tube wall.

Figure 12 summarizes the results for two design parameters, the thickness of the tube wall and the length of the calming section between the heaters and the boiling surface. Two different wall thicknesses were used with the 3" diameter boiling surface, .100 inch and .050 inch, and the length of the calming section was changed from 1" to 1/2". The results show that configuration using the .050" tube wall and the 1/2" calming section gives the least error (11%) at the center of the block.

From the analysis along with stress considerations for a tongue-in-groove joint, it was decided to set the thickness of the tube wall at .060 inch. However, the length of the calming section cannot be set until the assumption of constant temperature at the bottom of the calming section is checked. A computer program based on a two-dimensional model which allows for heat flow between and around the heater units is currently being checked out.

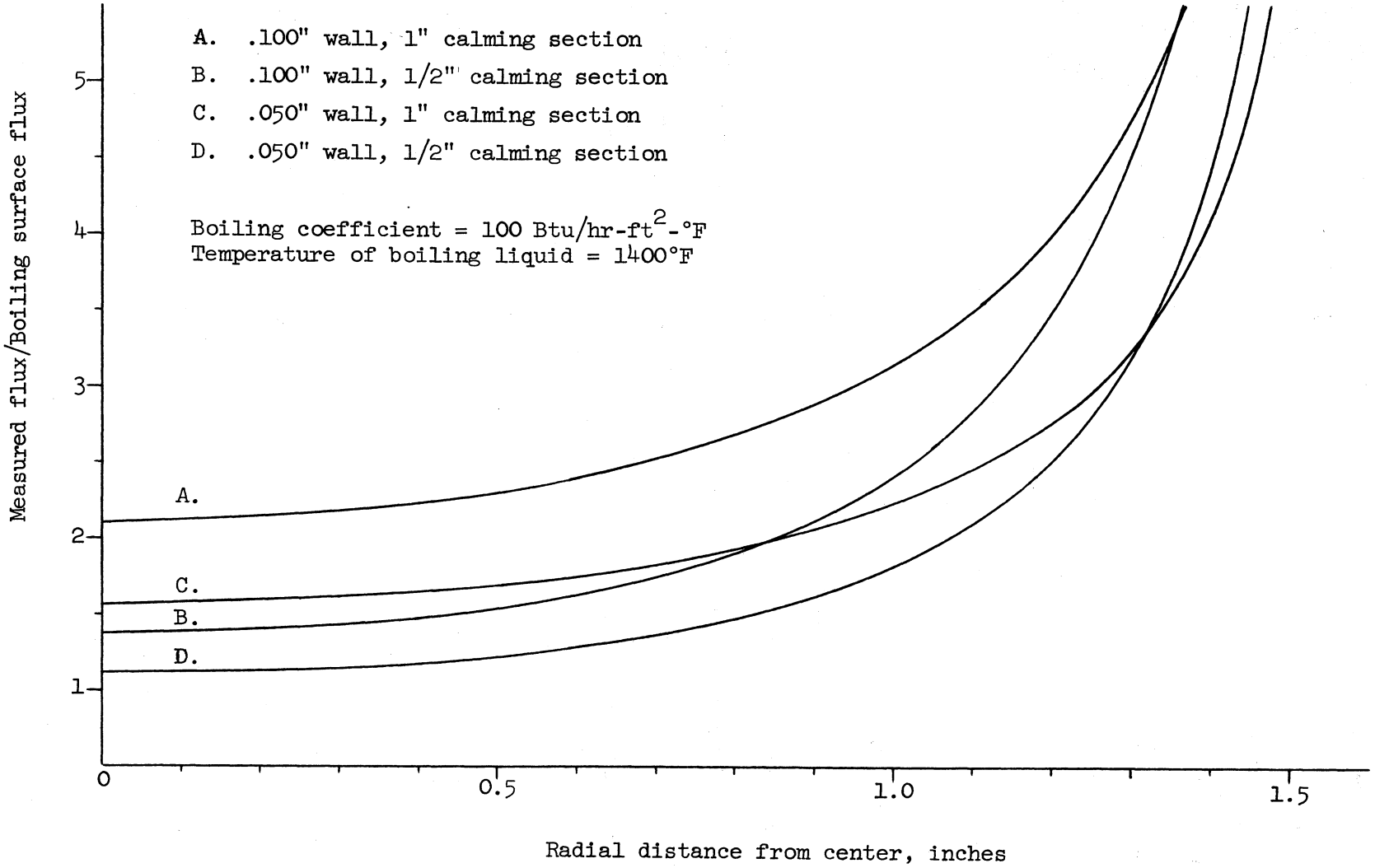

Figure 12. Analysis of Design Parameters for Proposed 3" Diameter Boiler

Forced Circulation Loop - Robert E. Barry

The objective of this program is to compare the two-phase heat transfer characteristics of liquid metals in swirl and straight-tube flow. The studies are to be carried out in the forced circulation loop constructed under Contract AF33(616)-8277. In this loop, potassium is preheated to a desired quality by means of external resistance heaters and then passed through a test section consisting of a length of 1/2-inch tube. Sodium vapor condensing on the outside of this tube is intended to supply a flux of up to 1-million Btu/hr-ft^2. A condenser, a cooler and a pump complete the circuit. (See Figure 13.)

After repeated operational problems due to plugging in the loop (as noted in the May QPR) the loop was disassembled between the inlets to the preheaters and the pump inlet and thoroughly cleaned. The hottrap was cleaned and charged with fresh zirconium chips and micrometallic filters were installed on a bypass charging line and on a bypass upstream of the pump. Reassembly was completed on July 6. On July 10 the loop was charged but circulation could not be obtained. The pump had plugged during the charging operation and the flowmeter and hottrap line had plugged soon afterward. Since the charged potassium had been filtered at 200°F, it is difficult to conceive of a mechanism for the formation of these plugs. The plugs in the flowmeter and the hottrap line were cleared by applying heat and pressure to the suspected location of the plug for long periods of time. The pumping section was heated by supplying power to the electromagnetic pump. Since the pump was plugged, the effect of this action was to heat the contents of the pumping section. All lines were clear by July 30. It is worth noting that this was the first time that the application of heat and pressure was successful in clearing a plug in the loop.

Some minor modifications were made to the loop and on August 8, the hot-

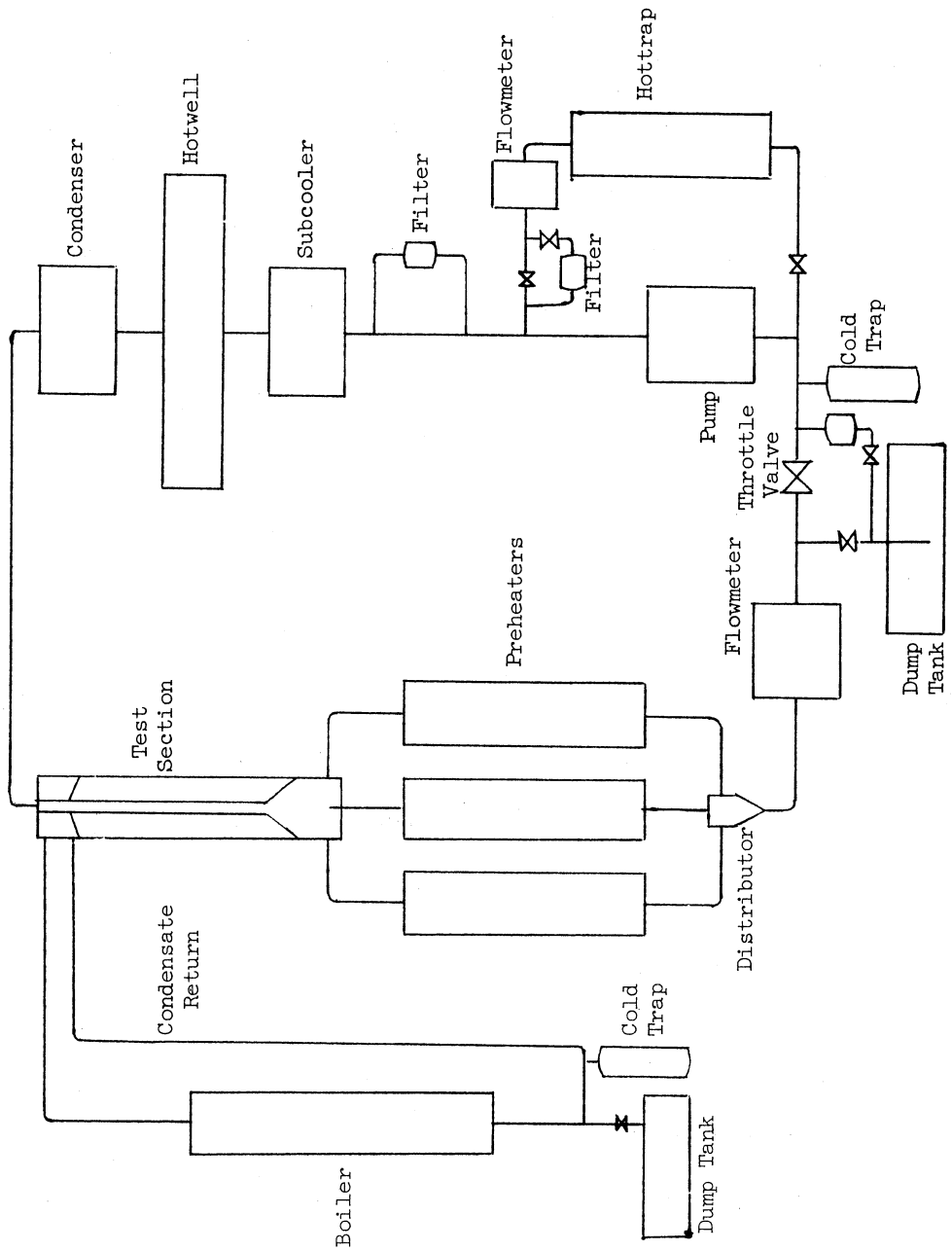

Figure 13. Forced Circulation Loop

trap was charged and circulation begun in the hottrap loop at 1.4 GPM and 800°F. Within an hour (the hottrap was at 1250°F and the pump at 940°F) a plug had developed in the pump cutting off circulation.

At present, attempts are being made to clear the pump as before by the application of successively higher power levels. To date no progress has been made in dislodging the plug.

It is now planned to obtain a new pump with a larger restriction in the pumping section. A style IV or VI pump will be obtained from MSA and used to circulate the potassium. The restriction in these pumps is 3 and 4 times larger than that in the style II presently in use. It is not known whether the present pump had been completely unplugged following earlier difficulties with metallic-type plugs. It may have been only partially opened thus permitting flow but being quite susceptible to plugging. It is felt that if oxygen contamination does exist within the system that it can be removed by a combination of cold filtering and hot trapping if circulation can be sustained for a sufficiently long period.

While awaiting a new pump it is planned to remove the present pump if the plug cannot be freed and attempt to clean it with a water-alcohol mixture. If the plug is not water soluble the pumping section will be removed and sectioned to reveal the nature and composition of the plug.

If the pump can be cleaned such that no restrictions exist in the channel, it will be reinstalled and operation initiated without the hottrap. (On repeated occasions stoppage has resulted following initiation of hottrapping procedures.) If flow can be sustained through the cold filter in the loop, the temperature level will be gradually raised to 1200°F. Attempts will then be made to operate the hottrap at temperatures up to 1000°F in order to minimize the oxygen concentration. This procedure parallels that used preceding the earlier studies during which two phase flow data was obtained.

Liquid Metal Boiling in Agravic Fields - Herman Merte

A number of tests had been conducted at a/g = 1 with 1/2 inch depth of mercury, at approximately 78 psia, in order to become familiar with the experimental procedures and operating characteristics of the apparatus prior to the high-g runs. In the early tests, upon bringing the system up to the desired operating heat flux, it was found that film boiling was established first, which then reverted to nucleate boiling. Figure 14 is a schematic of the test vessel showing the locations of the various thermocouples for reference in presenting the subsequent data.

Figure 15 shows the time-temperature data for a run, indicating the changes taking place from film to nucleate boiling. In order to detect any rapid changes which might take place a 20 point L & N recorder having variable range and zero suppression was incorporated to monitor continuously 10 of the more significant temperatures. For the more precise measurements appropriate selector switches are thrown and readings taken on the K-3 potentiometer.

In Figure 15, the power input to the heater was held constant equivalent to $q/A = 23{,}000$ Btu/hr-ft^2 at the heat transfer surface. The bulk liquid temperature (T-3) remains constant, being about 4°F subcooled, while the heater surface temperature rises and then suddenly drops. Accompanying this drop are increases in the vapor space temperature (T-4), ΔT(1-2) and ΔT water, which indicate increased heat transfer to the mercury with nucleate boiling. Similar behavior was observed by other workers (1) where apparent premature film boiling was attributed to the non-wetting characteristics of mercury. Data from the steady-state nucleate boiling conditions of Figure 15 are tabulated below:

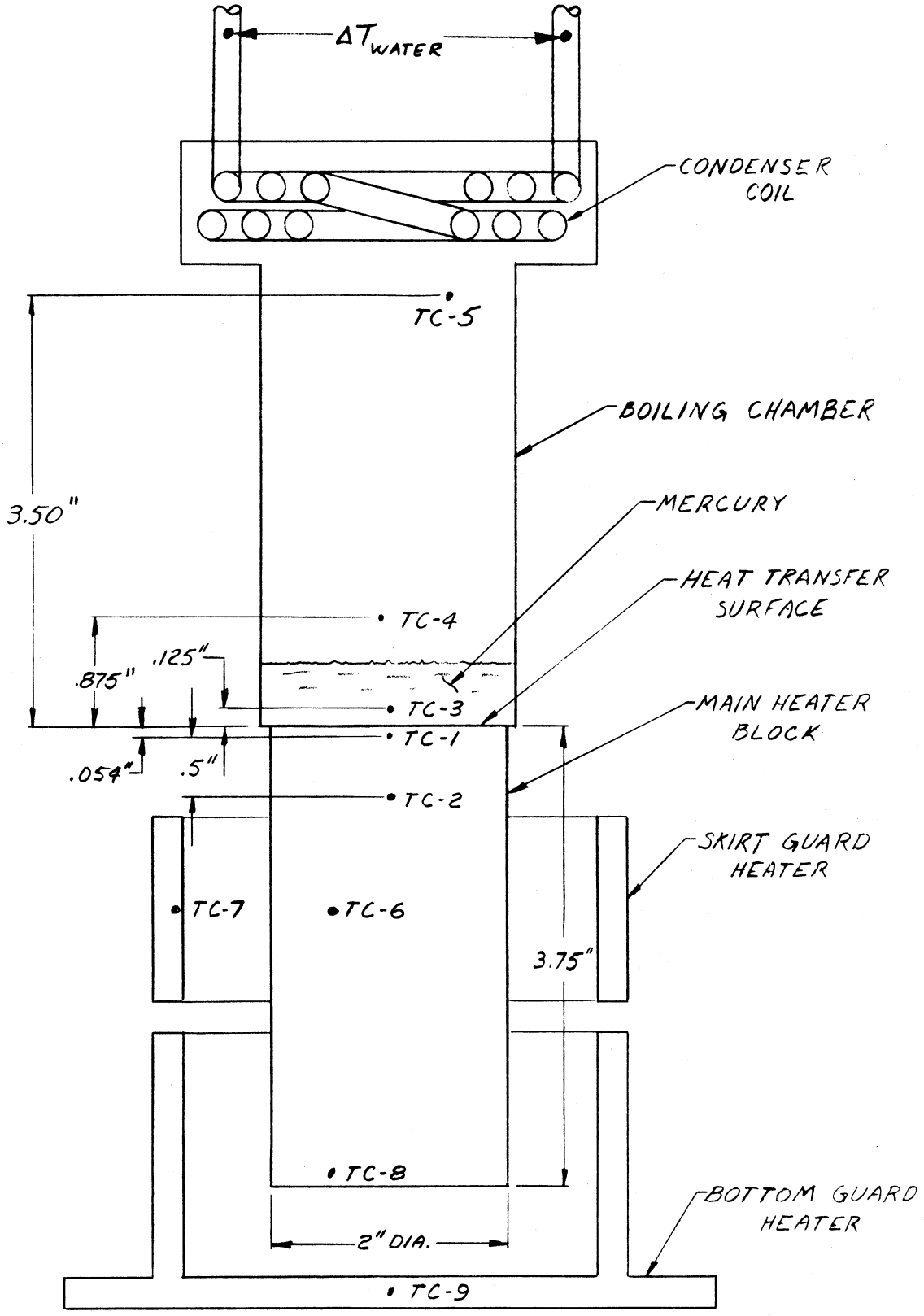

Figure 14. Thermocouple Locations for Reference

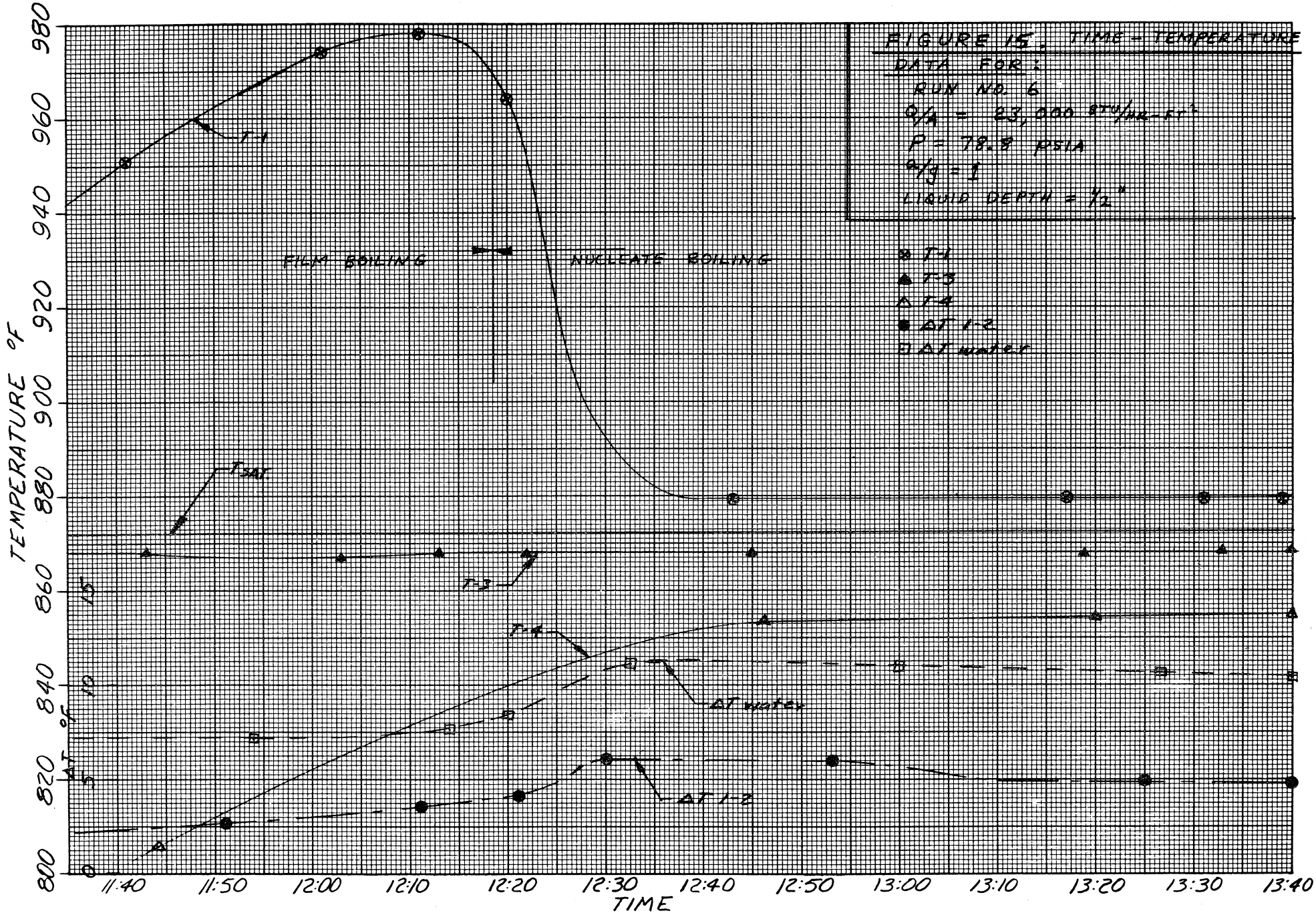
FIGURE 15 : TIME - TEMPERATURE DATA FOR :
RUN NO. 6
Q/A = 23,000 BTU/HR-FT²
P = 78.8 PSIA
Q/J = 1
LIQUID DEPTH = ½"
T-1
T-3
T-4
ΔT 1-2
ΔT water
FILM BOILING
NUCLEATE BOILING
T SAT
T-3
T-4
ΔT water
ΔT 1-2
TEMPERATURE °F
TIME
980
960
940
920
900
880
860
840
820
800
11:40
11:50
12:00
12:10
12:20
12:30
12:40
12:50
13:00
13:10
13:20
13:30
13:40
15
10
5
0
ΔT °F

Test Run No. 6 . a/g = 1

(1) $(q/A)_{EI}$ = 22,500 Btu/hr-ft^2

(2) $(q/A)_{\Delta T(1-2)}$ = 23,300 Btu/hr-ft^2

(3) $(q/A)_{\Delta T \text{ water}}$ = 25,400 Btu/hr-ft^2

T_{surf} = 878.8°F
T_{sat} = 872.2°F
} ΔT_{sat} = 6.6°F

Subcooling = 4.1°F

P = 78.8 psia

Liquid Level = 1/2 inch

The heat fluxes were computed as discussed in Reference (2), and the excellent agreement now present is due primarily to the operation of the lower guard heater, which previously had been defective.

Data for a higher heat flux with nucleate boiling is tabulated below:

Test Run No. 7 . a/g = 1

(1) $(q/A)_{EI}$ = 46,900 Btu/hr-ft^2

(2) $(q/A)_{\Delta T(1-2)}$ = 47,500 Btu/hr-ft^2

(3) $(q/A)_{\Delta T \text{ water}}$ = 43,600 Btu/hr-ft^2

T_{surf} = 895.8°F
T_{sat} = 872.2°F
} ΔT_{sat} = 23.6°F

Subcooling = 3.4°F

P = 78.8 psia

Liquid Level = 1/2 inch

Another test was conducted in order to establish the maximum heat flux for this system with nucleate boiling at a/g = 1. This was accomplished by raising the power level in small increments. In order to do so in a reason-

able length of time it was not possible to wait for time steady state at each level. Thus some care should be exercised in comparing these results to steady-state results. Figure 16 shows the data for the entire period, along with indications of the regimes of boiling present. The transition from nucleate to film boiling, or the maximum heat flux, is fairly well defined, and is accompanied by a pronounced increase in temperature level of the heater, even with a large decrease in heat flux. The temperature measurement in the vapor region near the cooling coil (T-5) dropped off-scale on the recorder, as might be expected with the decrease in vapor generation rate. To determine the approximate region of the minimum heat flux for film boiling, the heat flux was then reduced in small increments until the system reverted to nucleate boiling, as is indicated in Figure 16.

A summary of the results for periods closest to steady-state are given below:

Test Run No. 8 a/g = 1

P = 78.2 psia Mercury Depth = 1/2" T_{sat} = 871.6°F

Time	Data No. Fig.4		T-1	T-3	T_{surf} °F (Estim.)	ΔT_{sat} °F	Remarks
1:01	1	48,500	890.0	868	888.6	17.0	Nucleate Boiling
1:19	2	52,000	891.3	867	889.8	18.2	Nucleate Boiling
1:34	3	58,000	898.4	867	896.8	25.2	Nucleate Boiling
1:49	4	63,000	904.0	866	902.2	30.6	Burnout occurs within this region of heat flux
1:53		68,000	B.O. ≈910	866		B.O. ≈36	
2:11	5	27,000	1051.3	866	1050.7	179.1	- Stable film boiling Transition from minimum film to nucleate
2:19		23,000	Min. ≈1010	867		Min. ≈140	
2:27	6	23,000	876.1	867	875.6	4.0	Nucleate Boiling

The maximum heat flux occurs within the region q/A = 63,000 - 68,000 Btu/hr-ft^2 with ΔT_{sat} 36°F, and the minimum film boiling heat flux occurs within the region q/A = 23,000 - 27,000 Btu/hr-ft^2 with ΔT_{sat} 140°F. For comparison with the steady-state data of Runs 6 and 7, the data above are plotted on Figure 17.

The correlation of Noyes (3) based on Na data predicts a maximum heat flux for mercury of $(q/A)_{max} = 2.6 \times 10^6$ Btu/hr-ft^2 for the test conditions used. The gross discrepancy with the experimental results here may well be a consequence of the poor wetting of mercury with the type 347 stainless steel heating surface used.

With subsequent tests it was not possible to obtain nucleate boiling at all. Small amounts of Mg were added to the mercury, which was successful in producing nucleate boiling for short periods of time only. It was then planned that data be taken for film boiling at high acceleration with the view that long term operation may cause nucleate boiling once again. The cooling system was modified to use air as well as water, so that the liquid could be maintained at saturation conditions with the low heat flux associated with film boiling. The results for one run are tabulated below:

Test Run No. 17		
P = 80.3 psia Mercury Depth = .55" q/A = 18,000 Btu/hr-ft^2		
	a/g = 1	a/g = 5
T_{sat} (at Heater Surface)	875.3	877.2
ΔT_{sat} - °F	282	101
T_{liq} - °F	873.7	874.8
h - Btu/hr-ft^2 - °F	64	178

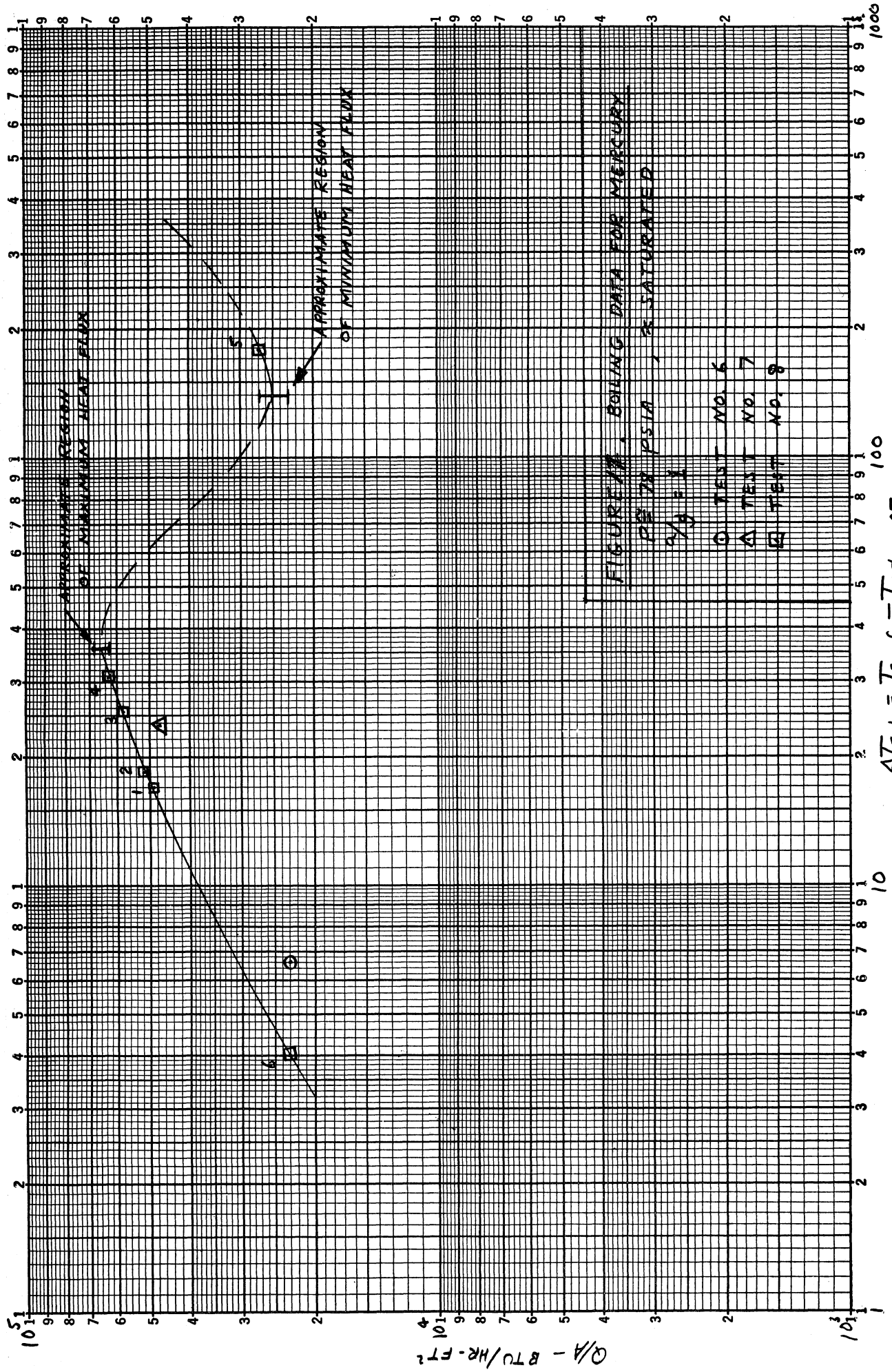
APPROXIMATE REGION OF MAXIMUM HEAT FLUX
APPROXIMATE REGION OF MINIMUM HEAT FLUX
FIGURE 14 - BOILING DATA FOR MERCURY AT 28 PSIA - 2" SATURATED
TEST - NO. 6
TEST - NO. 7
TEST - NO. 8
$\Delta T_{sat} = T_{surf} - T_{sat}$ °F
Q/A - BTU/HR-FT²

The increase in the heat transfer coefficient by a factor of almost 3 for a 5-fold increase in a/g is noted, although any general conclusions must await the availability of more data.

In conducting the next test, rather erratic behavior of the temperature measurements were noted. The equipment was cooled down and disassembled, and a slight crack had formed in the stainless steel foil adjacent to the heater surface causing mercury to leak out. The boiling surface itself had what appeared to be an oxide layer, perhaps MgO, adhering to it. This may have prohibited obtaining further nucleate boiling.

An attempt was made to attach a type 347 stainless steel foil .005 inches thick to the copper heater block to avoid further cracks, but this was not successful. Instead, a .005 inch foil of SAE 1010 low carbon steel was obtained and attached to the copper heater block to serve as the boiling surface. By copper plating the foil prior to contact with mercury, it was found that the surface was wet by the mercury after the copper was removed by amalgamation. The presence of the copper plating also improved the bonding of the steel foil to the copper block in the vacuum silver-brazing process used. The test vessel is now being reassembled.

LITERATURE CITED

1. Bonilla, C. F., et al, "Reactor Heat Transfer Conference of 1956," TID-7529 Part 1, Book 2, November 1957, pp. 324-341.

2. Balzhiser, R. E., et al, "Investigation of Liquid Metal Boiling Heat Transfer," 4th Quarterly Progress Report, 05750-12-P, May 1964.

3. Noyes, R. C., "An Experimental Study of Sodium Pool Boiling Heat Transfer," J. Heat Trans. ASME, Series C, Vol. 85, May 1963, pp. 125.

APPENDIX

A. Finite-difference approximation for Laplace's equation in cylindrical

For steady-state heat conduction,

Laplace's equation in cylindrical coordinates with polar symmetry is

$$\frac{\partial^2 T}{\partial r^2} + \frac{1}{r}\frac{\partial T}{\partial r} + \frac{\partial^2 T}{\partial Z^2} = 0$$

r = radial direction

Z = axial direction

To obtain the finite-difference approximations for the various derivatives, obtain Taylor series expansions around the general point $T_{i,j}$ where the subscript i indicates the axial direction and j indicates the radial direction.

In the axial direction,

$$T_{i,j+1} = T_{i,j} + \Delta r\left(\frac{\partial T}{\partial r}\right)_{i,j} + \frac{(\Delta r)^2}{2!}\left(\frac{\partial^2 T}{\partial r^2}\right)_{i,j} + \frac{(\Delta r)^3}{3!}\left(\frac{\partial^3 T}{\partial r^3}\right)_{i,j} + \ldots \qquad (1)$$

$$T_{i,j-1} = T_{i,j} - \Delta r\left(\frac{\partial T}{\partial r}\right)_{i,j} + \frac{(\Delta r)^2}{2!}\left(\frac{\partial^2 T}{\partial r^2}\right)_{i,j} - \frac{(\Delta r)^3}{3!}\left(\frac{\partial^3 T}{\partial r^3}\right)_{i,j} + \ldots \qquad (2)$$

Subtracting equation (2) from equation (1)

$$T_{i,j+1} - T_{i,j-1} = 2\left(\frac{\partial T}{\partial r}\right)_{i,j}\Delta r + \frac{2}{3!}\left(\frac{\partial^3 T}{\partial r^3}\right)_{i,j}(\Delta r)^3 + \ldots$$

$$\left(\frac{\partial T}{\partial r}\right)_{i,j} = \frac{T_{i,j+1} - T_{i,j-1}}{2\Delta r} + O(\Delta r)^2 \qquad (3)$$

Adding equation (1) and equation (2)

$$T_{i,j+1} + T_{i,j-1} = 2T_{i,j} + \frac{2}{2!}\left(\frac{\partial^2 T}{\partial r^2}\right)_{i,j}(\Delta r)^2 + \frac{2}{4!}(\Delta r)^4\left(\frac{\partial^4 T}{\partial r^4}\right)_{i,j} + \ldots$$

$$\left(\frac{\partial^2 T}{\partial r^2}\right)_{i,j} = \frac{T_{i,j+1} - 2T_{i,j} + T_{i,j-1}}{(\Delta r)^2} + O(\Delta r)^2 \qquad (4)$$

Similarly for the Taylor series expansions in the axial direction,

$$\left(\frac{\partial^2 T}{\partial Z^2}\right)_{i,j} = \frac{T_{i+1,j} - 2T_{i,j} + T_{i-1,j}}{(\Delta Z)^2} + O(\Delta Z)^2 \qquad (5)$$

Substituting equations (2), (3), and (4) into Laplace's equation and letting

$$Z = i\,\Delta Z \qquad i = 0, 1, 2, \ldots, M$$

$$r = j\,\Delta r \qquad j = 0, 1, 2, \ldots, N$$

$$\frac{T_{i,j+1} - 2T_{i,j} + T_{i,j-1}}{(\Delta r)^2} + \frac{1}{2j(\Delta r)^2}\left(T_{i,j+1} - T_{i,j-1}\right) + \frac{T_{i+1,j} - 2T_{i,j} + T_{i-1,j}}{(\Delta Z)^2} = 0$$

Multiplying through by $(\Delta r)^2$ and solving for $T_{i,j}$

$$T_{i,j} = \frac{\left(1 + \frac{1}{2_j}\right) T_{i,j+1} + \left(1 - \frac{1}{2_j}\right) T_{i,j-1} + \left(\frac{\Delta r}{\Delta Z}\right)^2 \left(T_{i+1,j} + T_{i-1,j}\right)}{2\left[1 + \left(\frac{\Delta r}{\Delta Z}\right)^2\right]}$$

B. Convection boundary condition

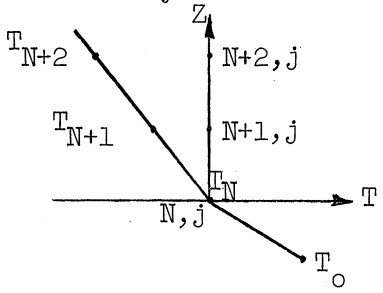

Expanding the points N+1 and N+2 around the boundary point N,

$$T_{N+1,j} = T_{Nj} + \Delta Z \left(\frac{\partial T}{\partial Z}\right)_{N,j} + \frac{(\Delta Z)^2}{2!}\left(\frac{\partial^2 T}{\partial Z^2}\right)_{N,j} + \frac{\Delta Z^3}{3!}\left(\frac{\partial^3 T}{\partial Z^3}\right)_{N,j} + \ldots \qquad (1)$$

$$T_{N+2,j} = T_{N,j} + 2\Delta Z \left(\frac{\partial T}{\partial Z}\right)_{N,j} + \frac{(2\Delta Z)^2}{2!}\left(\frac{\partial^2 T}{\partial Z^2}\right)_{N,j} + \frac{(2\Delta Z)^3}{3!}\left(\frac{\partial^3 T}{\partial Z^3}\right)_{N,j} + \ldots \qquad (2)$$

Multiplying equation (1) by 8 and subtracting equation (2) from the result,

$$8\,T_{N+1,j} - T_{N+2,j} = 7\,T_{N,j} + 6\,\Delta Z \left(\frac{\partial T}{\partial Z}\right)_{N,j} + 2(\Delta Z)^2\left(\frac{\partial^2 T}{\partial Z^2}\right)_{N,j} + O(\Delta Z)^4$$

However, $\left(\frac{\partial T}{\partial Z}\right)_{N,j} = \frac{h}{K}\left(T_{N,j} - T_o\right)$

Solving for $\frac{\partial^2 T}{\partial Z^2}$,

$$\frac{\partial^2 T}{\partial Z^2} = \frac{1}{2(\Delta Z)^2}\left[8\,T_{N+1,j} - T_{N+2,j} - 7\,T_{N,j} - 6\,\frac{\Delta Z h}{K}\left(T_{N,j} - T_o\right)\right] + O(\Delta Z)^2$$

Substituting into Laplace's equation and solving for $T_{N,j}$,

$$T_{N,j} = \frac{\left(1 + \frac{1}{2_j}\right) T_{N,j+1} + \left(1 - \frac{1}{2_j}\right) T_{N,j-1} + \frac{1}{2}\left(\frac{\Delta r}{\Delta Z}\right)^2 \left[8\,T_{N+1,j} - T_{N+2,j} + 6\,\frac{\Delta Z h}{K}\,T_o\right]}{2 + \frac{1}{2}\left(\frac{\Delta r}{\Delta Z}\right)^2 \left(7 + 6\,\frac{\Delta Z h}{K}\right)}$$

C. Pseudo convection coefficient for radiation

The heat flux between a surface at temperature T_1 and a surface at temperature T_2 is:

$$q/A = \sigma F(T_1^4 - T_2^4) = h_R(T_1 - T_2)$$

Therefore,

$$h_R = \sigma F \frac{(T_1^4 - T_2^4)}{T_1 - T_2} = \sigma F(T_1^2 + T_2^2)(T_1 + T_2)$$

$$h_R = \sigma F \frac{(T_1+T_2)}{2}\left[(T_1+T_2)^2 + (T_1-T_2)^2\right] = \sigma F \frac{(T_1+T_2)^3}{2}\left[1 + \left(\frac{T_1-T_2}{T_1+T_2}\right)^2\right]$$

Since $T_1 - T_2 = \Delta T$

and $\frac{T_1 + T_2}{2} = T_{avg}$

$$h_R = 4\sigma F\, T_{avg}^3 \left[1 + \left(\frac{\Delta T}{2\, T_{avg}}\right)^2\right]$$

D. Inside tube wall coefficients.

At some point above the boiling plate, the temperature of the tube wall will be equal to that of the liquid in contact with it. Neglecting radial gradients across the thickness of the tube wall, there will be no heat flow up the tube wall at this point. For an element of height ΔX_1, the energy into the bottom of the element is equal to the energy which is transferred across the inside wall due to boiling and the energy transferred across the outside wall due to radiation. If the temperature at the bottom of the element is assumed, these fluxes based on the average temperature of the element can be calculated, thus determining ΔX_1. The procedure is then repeated for the next element. Figure 18 illustrates the sequence of operations used for determining the length of an element. The boiling flux on the inside tube wall is determined from the postulated boiling curve given in Figure 19.

The results of the calculations are shown in Figure 20 where the temperature of the wall is given as a function of the distance along the tube wall. To use these results in the computer program for the test section, the height of the tube wall above the boiling plate is assumed. From Figure 20, temperatures along the inside tube wall can be determined and the boiling coefficients along the wall can be assigned using the postulated boiling curve, Figure 19. When the temperature field in the test section is determined by the computer, the temperature at the bottom of the tube wall at its junction with the boiling plate is checked. If this temperature does not correspond to the length of assumed tube wall, another length is assumed until agreement is reached.

FIGURE 18

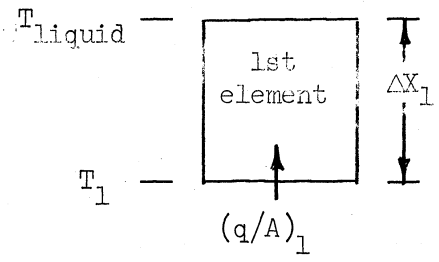

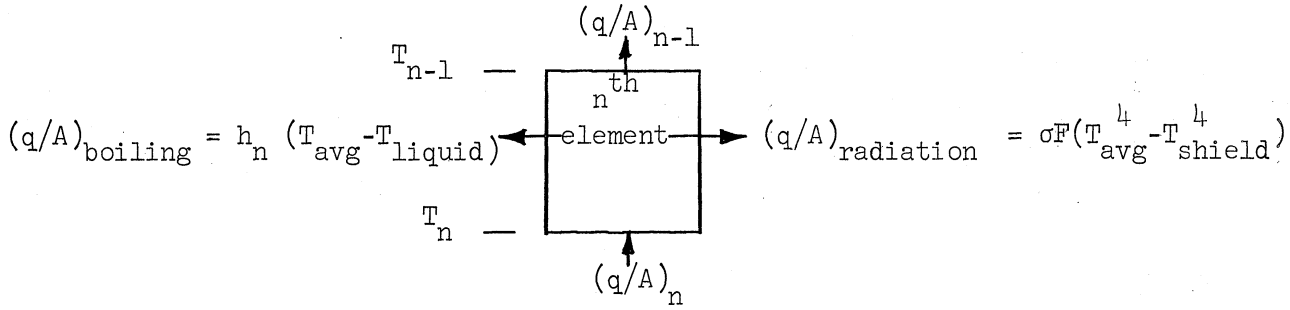

$T_{shield} = 1460°R$

$T_{liquid} = 1400°F$

1. Assume T_n
2. Determine $(q/A)_{boiling}$ based on $\frac{T_{n-1} + T_n}{2}$ from postulated boiling curve
3. Make a heat balance:

$$(q/A)_n A_{wall} = (q/A)_{boiling} A_{boiling} + (q/A)_{radiation} A_{radiation} + (q/A)_{n-1} A_{wall}$$

4. Assume that the total temperature drop $T_n - T_{n-1}$ occurs over the entire length of the element ΔX_n

$$(q/A)_n = \frac{K(T_n - T_{n-1})}{\Delta X_n}$$

5. Solve for ΔX_n

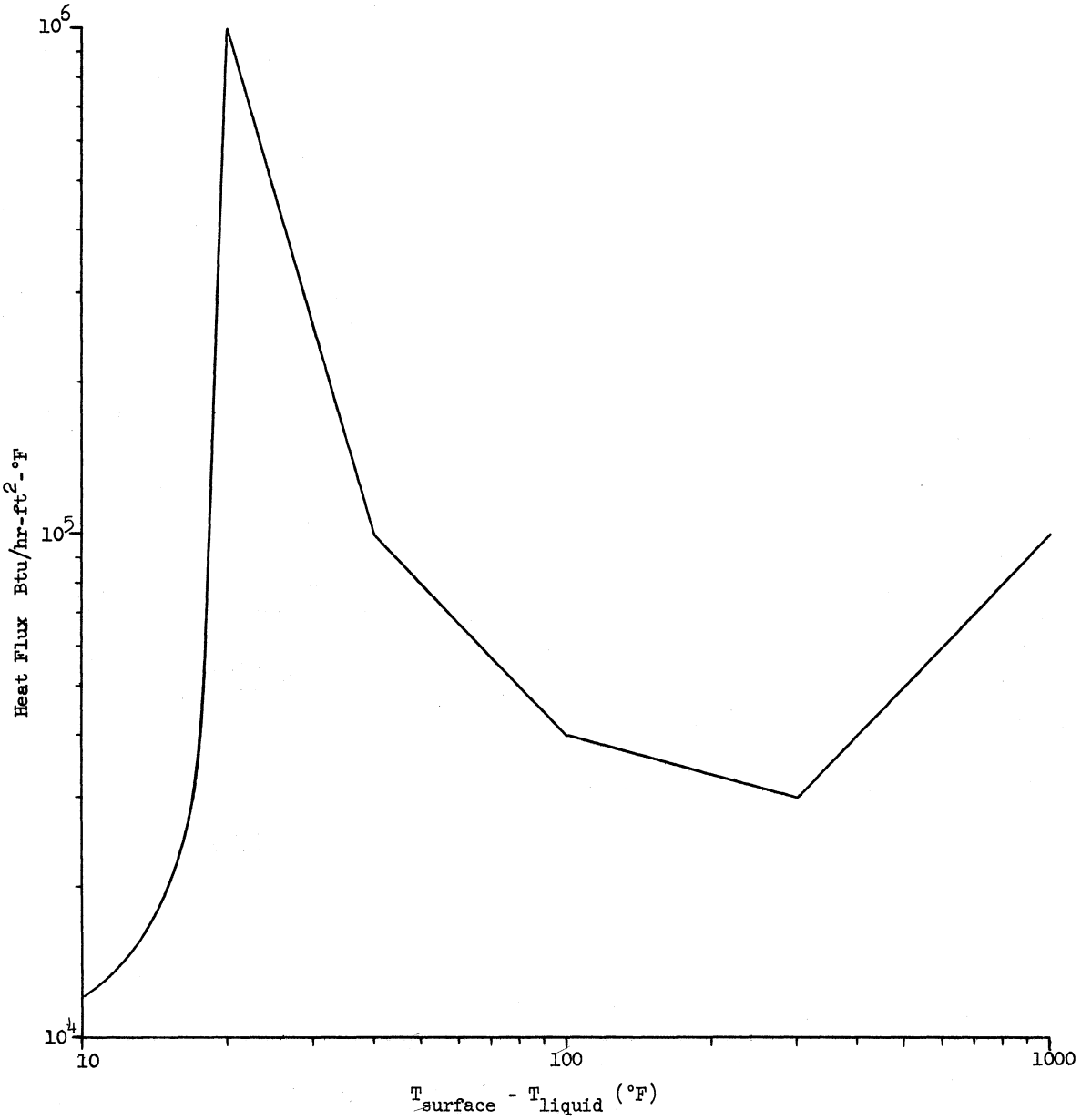

Figure 19. Postulated Boiling Curve for Assigning Inside Tube Wall Boiling Coefficients

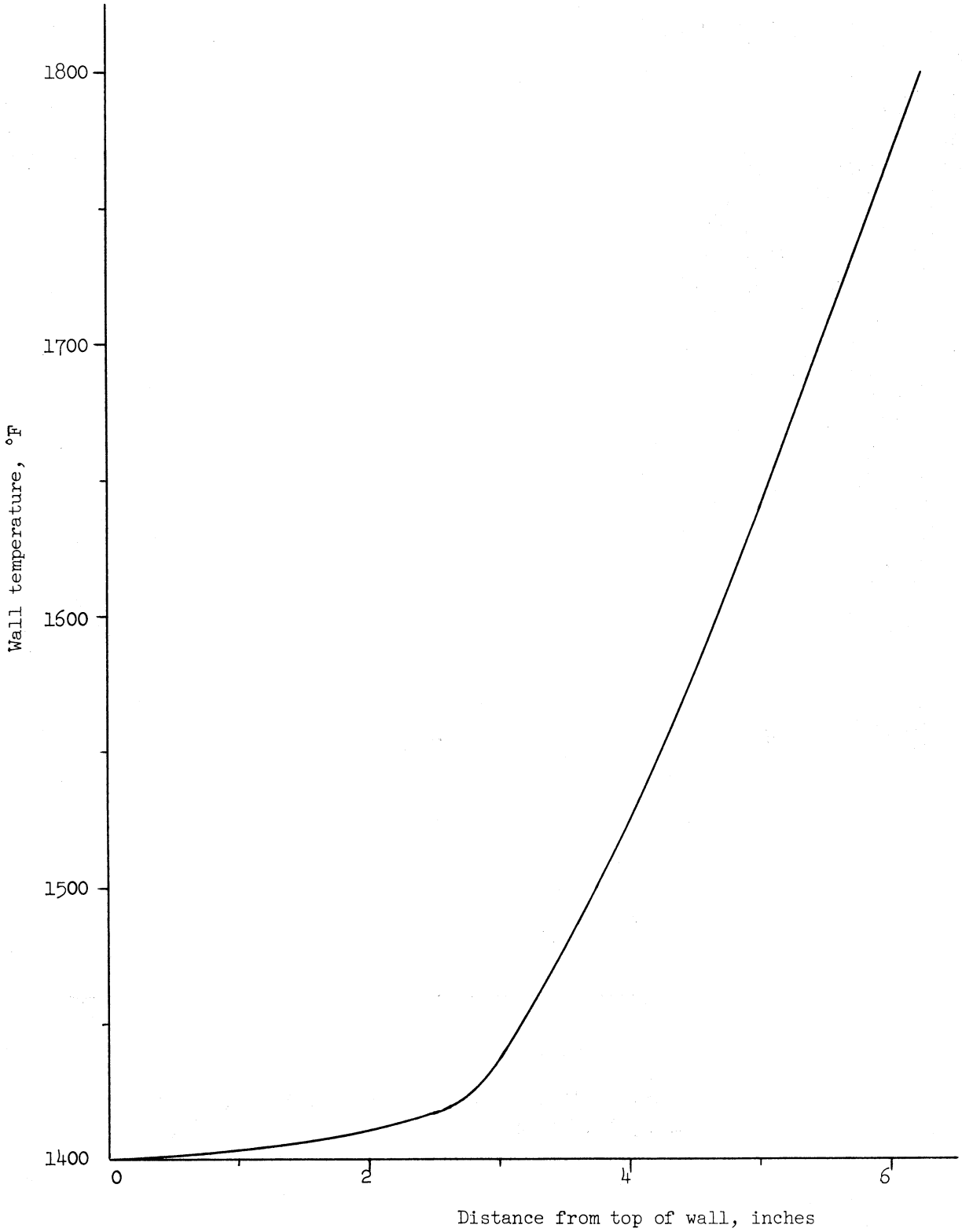

Figure 20. Longitudinal Variation of Wall Temperature